Journal of Materials Chemistry A

RSC Publishing

PAPER

View Article Online
View Journal | View Issue

Cite this: J. Mater. Chem. A, 2013, 1, 5081

How a bio-based epoxy monomer enhanced the properties of diglycidyl ether of bisphenol A (DGEBA)/graphene composites

Lijun Cao,[ab] Xiaoqing Liu,*[a] Haining Na,[a] Yonggang Wu,[b] Wenge Zheng[a] and Jin Zhu*[a]

Received 31st December 2012
Accepted 20th February 2013

DOI: 10.1039/c3ta01700a

www.rsc.org/MaterialsA

A bio-based epoxy monomer (GA-II) was synthesized from renewable gallic acid. The aromatic group contained made it capable of being absorbed onto the surface of graphene *via* strong π–π interactions, which was proven by Raman spectra and UV spectra. The GA-II anchored graphene was easily homogeneously dispersed in the epoxy resin. After solidification, the graphene/epoxy composites demonstrated superior performances in terms of good mechanical properties, excellent thermal conductivity, as well as high electrical conductivity. With the addition of only 2 wt% GA-II/graphene, the tensile strength, tensile modulus, flexural strength and flexural modulus of the composites were improved by 27%, 47%, 9% and 21%, respectively. The thermal and electrical conductivities were also improved by 12-fold (from 0.15 to 1.8 W m^{-1} K^{-1}) and 8 orders (from 7.0×10^{-15} to 3.28×10^{-5} s cm^{-1}), respectively. This work provided us with an environmentally friendly agent with high efficiency for graphene dispersion and demonstrated an efficient method for fabricating epoxy/graphene composites with superior properties.

1 Introduction

Graphene, characterized by a single-layered two-dimensional (2D) structure, has attracted tremendous attention in recent years due to its high values of aspect ratio, well-defined thermal conductivity, unique mechanical properties and excellent electrical properties.[1–5] It has been considered useful in various applications, such as memory devices,[4] hydrogen storage,[6] solar cells[7] and polymer composites.[8–10] As for its application in polymer composites, graphene is usually used as an effective inorganic filler to improve their electrical, thermal and/or mechanical properties.[1,8,11–14] However, due to the high surface area and strong van der Waals forces, graphene has a pronounced tendency to aggregate together and its predicted properties fail to be fully reached.[15–17] Therefore, many efforts have been made to improve its dispersion and interface interactions in polymer matrixes so as to demonstrate its nano-enhancement effect.

The functionalization methods of graphene could be summarized into two categories. One is covalent bonding and the other is non-covalent wrapping *via* π–π interactions. For the former method, a large number of polymer segments or reactive sites, such as polystyrene,[18] poly(*t*-butylacrylate)[19] and epoxides,[20] are usually employed to functionalize graphene *via* grafting-from or grafting-to approaches. For example, Fang *et al.* demonstrated an effective method to covalently graft polystyrene chains onto the surface of graphene sheets by diazonium addition/ATRP to prepare polystyrene composites with a prominent reinforcement effect.[21] S. Ganguli *et al.* prepared the epoxy composite filled with silane chemically functionalized graphene and an improved thermal conductivity was obtained.[22] Apparently, the grafting of polymer segments or reactive sites onto the graphene sheets could result in better dispersion and enhanced properties. However, these methods tend to alter, or even destroy, the desirable properties of graphene, especially its inherent electronic properties and thermal conductivity.[8] The non-covalent functionalization is based on van der Waals forces or π–π interactions between the surfactants and the sp^2 hybridized atoms of graphene, which is deemed to be a promising method to avoid defects and preserve almost all of its original characteristics. Many surfactants or polymers containing aromatic groups, such as poly(glycidyl methacrylate) containing localized pyrene groups (PyPGMA),[8] poly(methyl methacrylate),[23] polystyrene[1] and polyvinylpyrrolidone (PVP)[24] have been employed to functionalize or wrap graphene *via* π–π interactions using ultrasonic, solution mixing, melt blending or *in situ* polymerization.[1,4]

[a]Ningbo Key Laboratory of Polymer Materials, Ningbo Institute of Material Technology and Engineering, Chinese Academy of Sciences, 519 Zhuangshi Road, Zhenhai District, Ningbo 315201, China. E-mail: liuxq@nimte.ac.cn; jzhu@nimte.ac.cn; Fax: +86-574-86685186; Tel: +86-574-86685283

[b]College of Chemistry and Environmental Sciences, Hebei University, Baoding, Hebei 071002, China

In recent years, more and more attention has been paid to the bio-based materials because of the diminishing petroleum oil reserves and serious environment pollution.[25] The conversion of biomass to useful polymers or composites has considerable economical and environmental values. Tannic acid is a type of bio-based polyphenol found in oak bark and leaves. Due to the numerous phenol groups in the structure and its unique reducing characteristics, it has been used as a reducing agent or stabilizing agent for some nanoparticles.[26,27] Especially, it was found that tannic acid has a strong tendency to be absorbed onto the surface of carbon nanotubes *via* π–π interactions in organic solvents and the stable tannic acid-facilitated carbon nanotube suspensions could be obtained easily.[27] Inspired by these discoveries, we synthesized a bio-based epoxy monomer from a tannic acid derivative (gallic acid, Scheme 1) and it was used as a novel surfactant or stabilizer for graphene suspension. Then the epoxy/graphene composites were fabricated and their properties, such as mechanical properties, thermal and electrical conductivities, were investigated. The objective of this work is to provide a novel bio-based stabilizer with high efficiency for graphene dispersion and demonstrate an efficient method for fabricating graphene/epoxy composites with superior properties. We hope that the synthesized epoxy played dual roles in the epoxy composites: (1) promoting the dispersion of graphene in the epoxy matrix, (2) serving as a linkage between the graphene and epoxy network for properties promotion. Up to now, the bio-based high efficient dispersant for graphene dispersion has never been reported.

2 Experimental section

2.1 Raw materials

The graphene sheets were prepared according to the method described in Zheng's published paper.[28] The C/O ratio of the graphene was 13.2 and the specific surface area was about 700 $m^2\ g^{-1}$ measured with a Micromeritics ASAP 2010 analyzer (Norcross, GA) by the Brunauer–Emmett–Teller (BET) method. This result indicates that each graphene platelet was comprised of 3–4 individual graphene sheets on average.[29] Diglycidyl ether of bisphenol A, DER-331 (DGEBA) with an epoxy equivalent weight of 182–192 was bought from Dow chemical Inc (China). Gallic acid (GA), allyl bromide (C_3H_5Br), 1,2-cyclohexanedicarboxylic anhydride (HHPA), 2-ethyl-4-methylimidazole (2,4-EMI) and 3-chloroperoxybenzoic (MCPBA, 75%) were supplied by Aladdin Industrial Inc. 3-*tert*-Butyl-4-hydroxy-5-methylphenyl sulfide was obtained from Han Si Chemical Co., Ltd., Shanghai. Acetone (C_3H_6O), sodium chloride (NaCl), methanol (CH_3OH), potassium carbonate (K_2CO_3), sodium sulfite (Na_2SO_3), anhydrous magnesium sulfate ($MgSO_4$), sodium bicarbonate ($NaHCO_3$) and dichloromethane (CH_2Cl_2) were all from Sinopharm Chemical Reagent and used as received.

2.2 Synthesis of gallic acid-based epoxy resin (GA-II)

GA-II was synthesized using a two-step process as shown in Scheme 1. The first step is the synthesis of allylated gallic acid (GA-I): 3 g GA, 24 g K_2CO_3 together with 25 mL C_3H_6O which were added into a 100 mL three necked round-bottom flask with a reflux condenser and mixed by vigorous stirring for 10 min. Then, the solution of 17 g C_3H_5Br in 25 mL acetone was slowly added over a period of 30 min before the mixture was heated to 70 °C and maintained at this temperature for another 24 h. The resulting product was cooled to room temperature and filtered before the acetone was removed by rotary evaporation. Finally, the crude product was dissolved in a certain amount of dichloromethane (CH_2Cl_2) and washed with saturated brine solution. The dichloromethane layer was concentrated by rotary evaporator and dried at 60 °C in vacuum oven for 12 h to get the GA-I product weighing 5.24 g (yield 90%).[30]

The second-step is the synthesis of gallic acid-based epoxy resin (GA-II):[31,32] the obtained allylated gallic acid was dissolved in 50 mL dichloromethane before 12.5 g *m*-CPBA and 0.14 g 3-*tert*-butyl-4-hydroxy-5-methylphenylsulphide were added. After the mixture was reacted at 40 °C for 48 h, it was cooled to −5 °C and kept at this temperature for 6 h. Then, the solid precipitation was removed *via* filtration and the filtrate was washed with a solution of 10% sodium sulfite, 5% aqueous solution of Na_2CO_3 and saturated aqueous solution of NaCl. The residual water in the organic layer was removed by anhydrous magnesium sulfate and the dichloromethane was removed by rotary evaporator. The obtained solid product was dissolved in 5 mL CH_2Cl_2 and poured into a 10-fold excess of cold methanol to get the precipitation. At last, the precipitation was collected *via* filtration and dried at 30 °C in a vacuum for 48 h. Then the pure product GA-II weighing 4.2 g was obtained (yield 80%). The epoxy value of GA-II determined by the chlorhydric acid–acetone method was about 0.93 and the calculated value was 1.01.

GA-I: ^1H NMR (CD_3Cl, δ ppm) 7.30 (s. 2H), 6.01–3.07 (m, 4H), 5.16–5.45 (m, 8H), 4.78–4.80 (m, 2H), 4.61–4.62 (m, 6H); ^{13}C

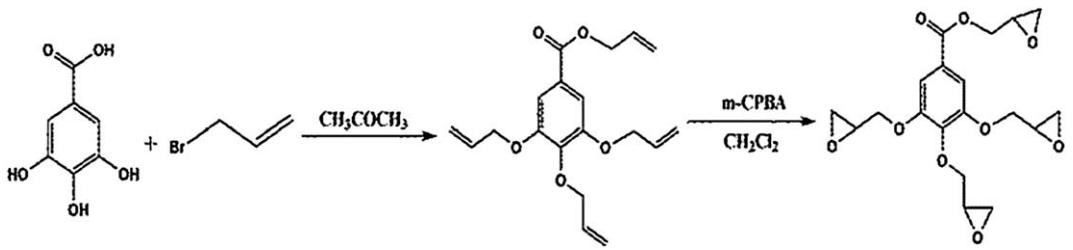

Scheme 1 Reaction route for the synthesis of gallic acid-based epoxy (GA-II).

NMR (CD_3Cl, δ ppm) 165.80, 152.59, 141.98, 134.19, 132.97, 132.28, 125.00, 118.18, 117.89, 117.69, 108.84, 74.06, 69.96, 65.62. FT-IR (cm^{-1}) 3081, 1646, 1384, 1207, 1112, 989, 927, 765.

GA-II: ^1H NMR (CD_3Cl, δ ppm) 7.33–7.40 (m, 2H), 4.00–4.67 (m, 8H), 3.32–3.48 (m, 4H), 2.71–2.90 (m, 8H); ^{13}C NMR (CD_3Cl, δ ppm), 165.54, 152.13, 142.52, 125.03, 109.55, 109.51, 74.25, 70.26, 65.757, 50.54, 50.01, 49.46. FT-IR (cm^{-1}) 3357, 3302, 2925, 1504, 1432, 1200, 1004, 867.

2.3 Fabrication of the GA-II functionalized graphene dispersion

0.50 g of graphene sheet together with 0.50 g GA-II were dispersed in 50 mL CH_2Cl_2 in a 650 W ice bath sonicator for 2 h. The dispersion was stable and no obvious precipitates were observed after it was centrifuged at a speed of 6000 revolutions per minute (rpm). The resulting suspension was ready for AFM, UV and Raman spectra characterization, as well as the preparation of the composites.

2.4 Preparation of the graphene/epoxy composites

The epoxy/graphene composites were fabricated by the following procedure: into the graphene CH_2Cl_2 dispersion obtained by the above method, the desirable epoxy resin (DER-331) together with a predetermined curing agent HHPA (epoxy and curing agent were in a 1 : 0.8 equivalent ratio) and 2,4-EMI (1 wt% on the basis of the total weight of HHPA and epoxy) were added. In order to achieve good mixing the mixture was sonicated at 100 W in an ice bath for 10 min before the solvent was removed under vacuum at 50 °C. The solvent-free mixture was transferred into a mold with cavity dimensions of 3 × 10 × 60 mm. The curing reaction was conducted at 60 °C for 2 h, 120 °C for 2 h and 180 °C for 2 h. The cured sample was left still at room temperature for 12 h prior to the property tests.

The different composites were named as neat epoxy, Modi. 0.25%, Modi. 0.5%, Unmodi. 0.5%, Modi. 1.0% and Modi. 2.0%, respectively (Table 1). Obviously, the nomination was based on the loading content of graphene in the composites. "Modi." in the sample code is used for the graphene modified by GA-II. "Unmodi." stands for the pristine graphene. The percentage following "Modi." and "Unmodi." represents the loading content of graphene. For example, "Modi. 1.0%" represents the composite containing 1.0 wt% graphene modified by GA-II. "Neat epoxy" stands for the cured epoxy resin without any graphene addition.

2.5 Characterization

The ^1H NMR and ^{13}C NMR spectra were recorded on a Bruker AVANCE III 400M nuclear magnetic resonance spectrometer in $CDCl_3$. The FT-IR spectrum (KBr) was collected with a Thermo Nicolet Nexus 6700 instrument. AFM was conducted on a Veeco Multimode V scanning probe microscope in a tapping mode. Raman spectra was recorded with a LabRam I confocal Raman spectrometer (France) using the wavelength of 632.8 nm. The ultraviolet-visible (UV-vis) spectroscopy using a computer-controlled spectrophotometer (Perkin-Elmer Lambda 950) were used to characterize the interaction between GA-II and graphene in dichloromethane (CH_2Cl_2). The morphology of graphene and its composites were investigated by a Tecnai G2 F20 transmission electron microscopy (TEM) at the accelerating voltage of 200 kV. Five to ten samples from each graphene/epoxy composite were tested to show the mechanical properties. The tensile test was performed at a cross-head speed of 0.5 mm min^{-1} followed ASTM D638. Flexural properties were measured according to ASTM D790 at a span-to-thickness ratio of 16 with the crosshead rate of 1.4 mm min^{-1}. Thermal conductivity was measured by a Netzsch LFA 457 laser flash thermal diffusivity apparatus according to ASTM DE1461-92 at room temperature. The volume resistivity was measured at room temperature using an Agilent 34401A digital multimeter and a YOOGAWA 7651 voltage source by the two-probe method. A three-terminal fixture (two electrode plus guard) proposed by the ASTM D257 for volume conductance determination of flat samples was used for the low conductance measurement. The sample was coated with silver paste on the surface to reduce the contact resistance between the sample and electrodes. The density of the graphene and epoxy matrix were respectively set as 2.28 g $cm^{-3}$and 1.1 g cm^{-3} for conversion from wt% to vol%.[12]

3 Results and discussion

3.1 Synthesis of gallic acid-based epoxy resin (GA-II)

As we know the reaction between organic acid and excess epichlorohydrin with sodium hydride as the basification reagent usually results in the epoxy oligomer, rather than the epoxy monomer. Therefore, in order to prepare the bio-based epoxy monomer from gallic acid, the two-step synthesis method shown in Scheme 1 was employed. The first step was the allylation of gallic acid in the presence of C_3H_5Br and K_2CO_3. Then the resulting terminal double bonds in GA-I were

Table 1 Mechanical properties of the epoxy/graphene composites

Sample	Tensile strength (MPa)	Tensile modulus (MPa)	Flexural strength (MPa)	Flexural modulus (MPa)
Neat epoxy	66(±3)	1970(±56)	128(±4)	3050(±60)
Modi. 0.25%	69(±4)	2580(±78)	136(±4)	3150(±70)
Unmodi. 0.5%	62(±3)	2440(±77)	82(±3)	2880(±70)
Modi. 0.5%	78(±4)	2680(±84)	138(±2)	3400(±40)
Modi. 1.0%	80(±2)	2820(±60)	139(±5)	3600(±50)
Modi. 2.0%	84(±3)	2890(±113)	139(±4)	3700(±30)

oxidized into epoxy groups with the help of *m*-CPBA in the following second step. In the previous literature,[33,34] this reaction was studied in much more detail and HPLC was used to separate the four isomers. In our experiment, the decomposition of 3-chloroperoxybenzoic (*m*-CPBA), which acted as the oxidizing agent, was suppressed in the presence of 3-*tert*-butyl-4-hydroxy-5-methylphenylsulphide.[31] This led to a higher conversion yield from double bond to epoxide. The reaction yield was as high as 80%.

The chemical structures of GA-I and GA-II were confirmed by NMR and FT-IR. In Fig. 1 the broad absorption peak of COOH or OH from 3000–3500 cm^{-1} for GA almost disappeared after the allylation of GA-I. Also, strong absorption bands at 1587 cm^{-1} and 1207 cm^{-1} were recognized and easily identified as the stretching vibration of the double bond and ester group in GA-I. After the epoxidation, the characteristic peaks at 3357 cm^{-1}, 3002 cm^{-1} and 1200 cm^{-1} for oxirene appeared. In order to further identify their structures, the NMR spectra are also shown in Fig. 2. In Fig. 2(a1), the peaks from 7.33 to 7.40 ppm were attributed to the protons attached on the benzene ring and the signals from 5.20 to 5.45 ppm, 6.01 to 6.07 ppm were assigned to the protons of –CH(2)═CH_2(1). The ^{13}C NMR spectrum shown in Fig. 2(a2) further supports the allylation of gallic acid, which exhibited the characteristic peaks for a double carbon bond at 132.3 ppm, 134.2 ppm and 117 ppm. In Fig. 2(b1), the signals from 4.00 ppm to 4.80 ppm were all attributed to the protons of H_4, $H_{4'}$, $H_{4''}$, H_5, $H_{5'}$ and $H_{5''}$, which were the characteristic peaks for methylene in glycidyl ester or glycidyl ether. Compared with Fig. 2(a2), the characteristic peaks for the unsaturated double carbon bond (132.3, 134.2 and 117 ppm) disappeared and the signals from 40 ppm to 50 ppm for the appearance of oxirene were noticed. These results indicated that the target compounds were synthesized successfully and the two-step method was an efficient way to prepare the epoxy monomer from gallic acid.

3.2 Fabrication and characterization of the GA-II functionalized graphene suspension

Graphene usually shows a G band at 1600 cm^{-1} and a D band at 1400 cm^{-1} on the Raman spectra. The G band is assigned to the in-plane bonding stretching motion of sp^2 carbon atoms and the D band is related to the breathing mode near the K zone boundary and ascribed to the edge of graphene.[32] Previous studies have demonstrated that the G band peak is shown at lower frequencies for electron donor dopants and at higher frequencies for electron acceptor dopants,[35,36] which is similar to that of carbon nanotubes.[37–39] In this work, the graphene was dispersed in CH_2Cl_2 by sonication together with GA-II. In order to investigate the interaction between GA-II and graphene sheet, the dispersion of GA-II functionalized graphene (GA-II/graphene) was investigated by Raman spectrometer. Fig. 3 is the Raman spectra of the GA-II/graphene suspension. Obviously, the G band was red shifted from 1592 cm^{-1} for graphene to 1589 cm^{-1} for GA-II/graphene. This shift provided the evidence for a charge transfer between the graphene sheet and GA-II molecule.[26,40,41] The I(D)/I(G) ratio of GA-II/graphene was decreased to 1.01 from 1.24 for graphene, which indicated that numerous small sp^2 domains were formed by GA-II modification.[42]

The UV-vis spectra of GA-II, GA-II/graphene and graphene in CH_2Cl_2 are shown in Fig. 4, which indicates the direct evidence for the π–π interaction between graphene and the GA-II. The absorption peak located at 266 nm was assigned to the n–π* electron transition in GA-II.[26,43,44] However, in the suspension of the GA-II/graphene system, the peak for the n–π* transition was blue shifted to 261 nm. This result also indicated the π–π interaction between graphene and GA-II.

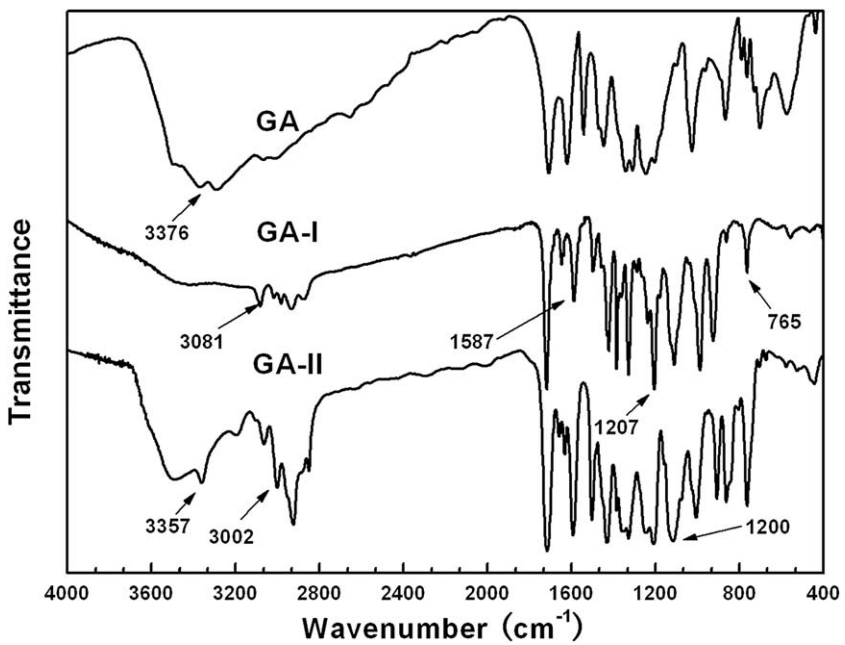

Fig. 1 FT-IR spectra of GA, GA-I, GA-II.

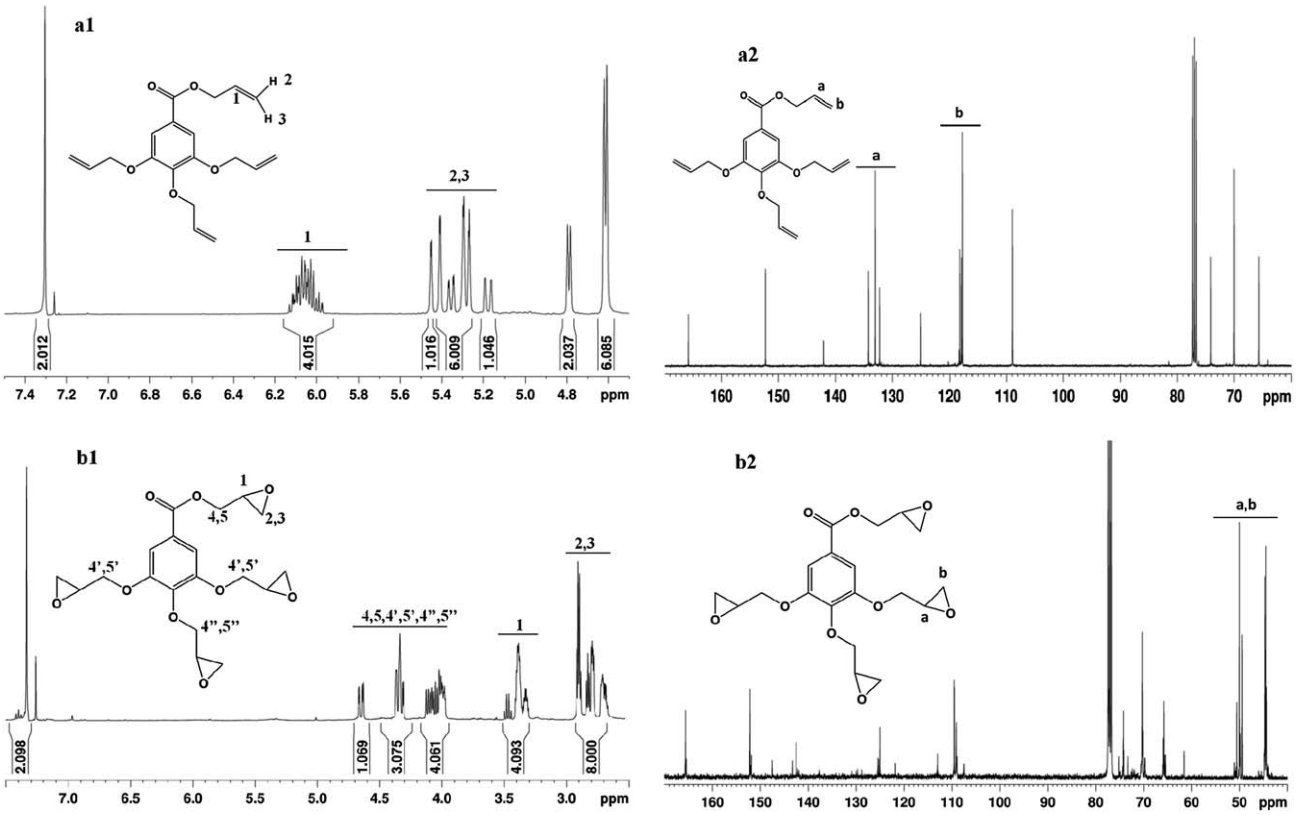

Fig. 2 ^{1}H NMR spectra of GA-I (a1), GA-II (b1) and ^{13}C NMR spectra of GA-I (a1), GA-II (b2).

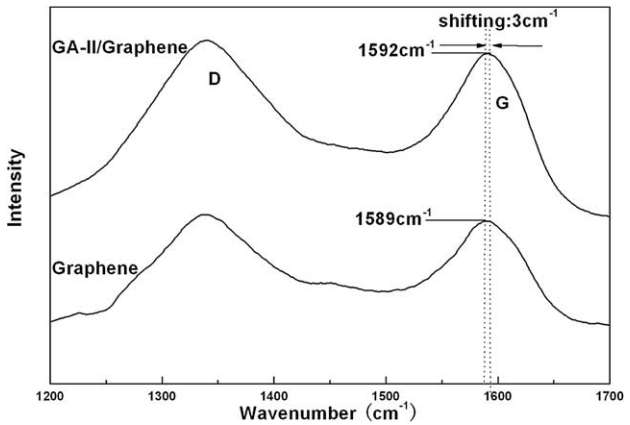

Fig. 3 Raman spectra of graphene and the GA-II/graphene suspension.

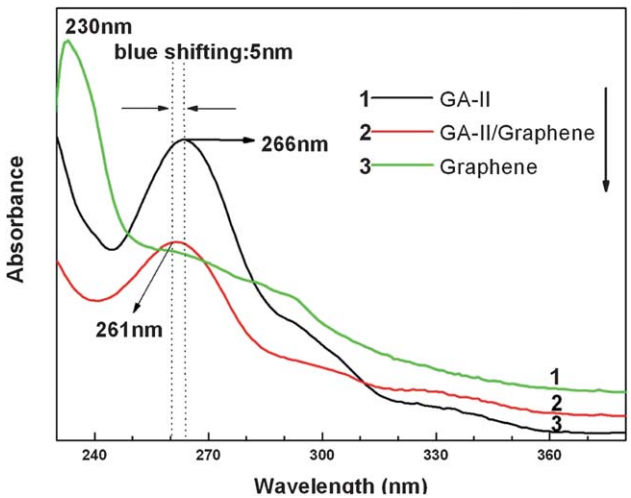

Fig. 4 UV-vis spectra of the GA-II, GA-II/graphene and graphene suspension.

In order to characterize the dispersion state of GA-II/graphene in CH_2Cl_2 and so as to further investigate the π–π interaction between GA-II and graphene, atomic force microscopy (AFM) and transmission electron microscopy (TEM) observation were also applied and the results are shown in Fig. 5. According to the AFM photo (Fig. 5a), it could be seen that the lateral size of the modified graphene sheets was about several micrometres and their average thickness was about 2.0 nm, indicating that the graphene sheets were almost exfoliated. The nano-layer was a little thicker than the single graphene, which might be due to the fact that the GA-II molecules were anchored on the surface of graphene. Fig. 5b shows a typical TEM micrograph of pristine graphene, which looks like a thin film with a wrinkled surface. After being modified by GA-II, the graphene layer appeared more transparent, as shown in Fig. 5c. These results also demonstrated that the graphene sheets were almost exfoliated and the agglomeration was prevented by the anchored GA-II molecules.[26]

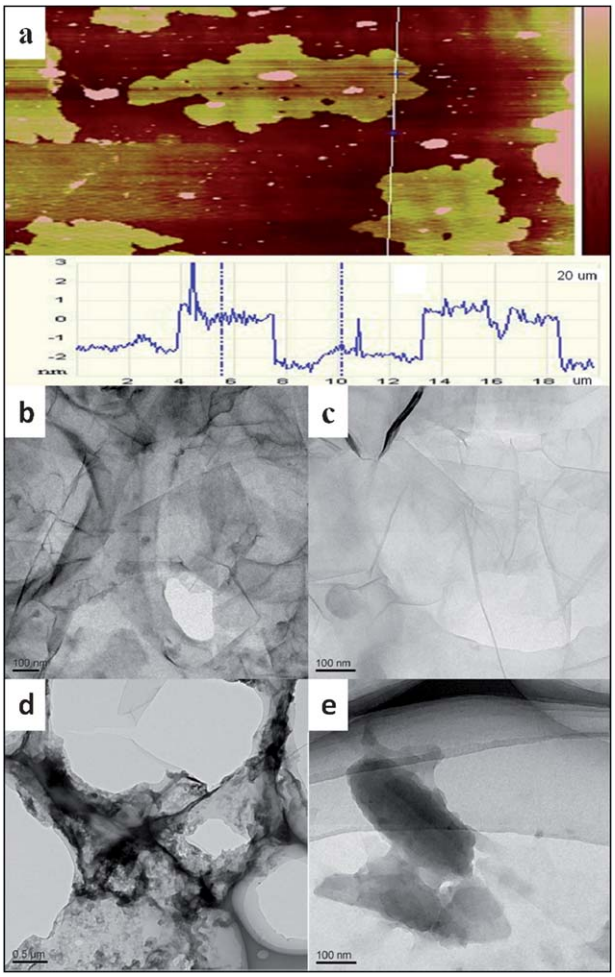

Fig. 5 A typical AFM image of GA-II/graphene (a), typical TEM images of pristine graphene (b) and GA-II/graphene (c) deposited on a substrate from the solution suspension, and TEM images for the GA-II/graphene dispersed in epoxy matrix (d and e).

3.3 Mechanical properties of the graphene/epoxy composites

It is well known that a small amount of graphene uniformly dispersed in the polymer matrix will increase its mechanical properties significantly. The mechanical testing of the composites was carried out and the results are summarized in Table 1. Comparing the data for Unmodi. 0.50% with that of the neat epoxy, it is easy to note that the tensile and flexural properties were decreased seriously with the addition of 0.50 wt% pristine graphene. However, after the graphene sheets were functionalized by GA-II, they played positive role in the mechanical reinforcement. With only 1 wt% GA-II/graphene addition, the tensile strength, tensile modulus and flexural strength were increased about 28% (from 66 MPa to 80 MPa), 43% (from 1970 MPa to 2820 MPa) and 21% (from 3050 MPa to 3700 MPa), respectively. When the content of GA-II/graphene was increased, their mechanical properties were increased further.

The mechanical properties of polymer/graphene composites are mostly dependent on the dispersion of graphene in the matrix, as well as the efficiency of the load transfer at the interface between graphene and polymers. In this work, the bio-based epoxy monomer GA-II was proven to have the capability to be adsorbed onto the surface of graphene *via* π–π interactions and the strong van der Waals forces among the individual graphene sheets were overcome, which revealed an expected good dispersion of graphene in the resulting epoxy composites. Fig. 5d and e show the TEM images of the epoxy/graphene composite in this study. Apparently, the GA-II/graphene particles were dispersed uniformly in the epoxy matrix. In addition, GA-II in fact was an epoxy monomer and it could easily chemically bond with the curing agent, which provided a strong surface adhesion between graphene and the epoxy matrix. Based on the above results, the conclusion that the synthesized bio-based epoxy monomer played dual roles in the composites could be drawn. One role is promoting the dispersion of graphene in the matrix *via* π–π interactions and the other is serving as a linkage between graphene and the epoxy matrix for the properties promotion. This was the reason for the significant mechanical properties enhancement in our study.

3.4 Thermal properties of the epoxy/graphene composites

The good dispersion of carbon materials, such as carbon fibers, carbon nanotubes or graphene, usually results in the thermal conductivity promotion of composite materials. In order to investigate the effect of graphene on the thermal properties of epoxy, the thermal conductivities of epoxy/graphene composites as a function of graphene loading content is shown in Fig. 6. As expected, the addition of GA-II/graphene enhanced the thermal conductivity of the epoxy resin significantly. With the addition of 0.5 wt% GA-II/graphene, the thermal conductivity was increased from 0.15 W m^{-1} K^{-1} for neat epoxy to 0.61 W m^{-1} K^{-1} for Modi. 0.5%, a 4-fold improvement. As the concentration of GA-II/graphene was further increased to 2 wt%, the thermal conductivity was improved by 12-fold, from 0.15 W m^{-1} K^{-1} to 1.8 W m^{-1} K^{-1}. When comparing the sample of Modi. 0.5% with that of Unmodi. 0.5%, it was noticed that the addition of 0.5 wt% untreated graphene barely changed the thermal conductivity. It was only about 0.17 W m^{-1} K^{-1}, similar to that

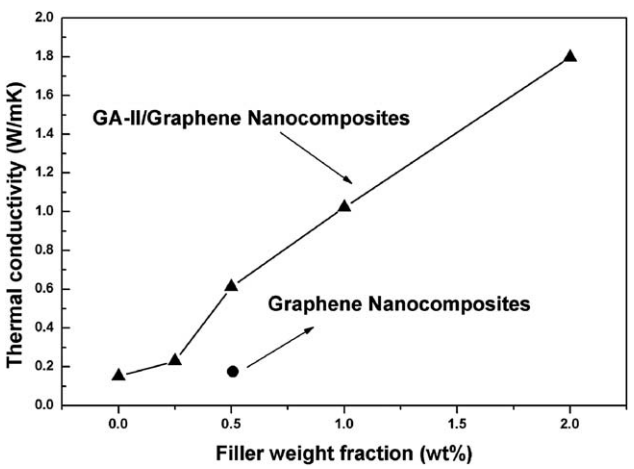

Fig. 6 Thermal conductivity plot for the epoxy/graphene composites.

of the neat epoxy. This might be due to the fact that the increase of thermal conductivity was also heavily dependent on the dispersion of graphene and the strong interfacial interaction between the nanofillers and polymer matrix.

Up to now, several reasons have been proposed to explain the thermal conductivity enhancement of graphene composites.[8,22] In this study, the following three reasons might be responsible for the significant enhancement: (i) the graphene with better integrity possessed better thermal conductivity. The non-covalent functionalization of the graphene sheet by GA-II preserved almost all of its original characteristics, including excellent thermal conductivity; (ii) the epoxy groups on GA-II generated covalent bonds with the epoxy matrix and formed the cross-linking structure of the epoxy/graphene composites, which strengthened the interfacial interaction between graphene and the epoxy matrix considerably. The strong interaction between the nanofillers and polymer could reduce the thermal interfacial resistance effectively and improve the phonon transport in the composite; (iii) the homogeneous dispersion of GA-II/graphene sheets in epoxy composites resulted in an increased contact surface area between the graphene and polymer, which promoted the heat flow and phonon diffusion in the epoxy/graphene composites.

3.5 Electrical properties of epoxy/graphene composites

Fig. 7 shows the electrical conductivity of the epoxy/graphene composites as a function of the filler volume fraction. It is noted that the electrical conductivity of the composite was significantly improved with the increase of graphene volume fraction. For the GA-II/graphene filled composites, the electrical conductivity was quickly increased from 7.0×10^{-15} S cm^{-1} for the neat epoxy to 1.37×10^{-9} S cm^{-1} for the Modi. 0.25%, with only a content of 0.121 vol% addition. At 2.0 wt% GA-II/graphene content (about 0.94 vol% of the composite), the conductivity was increased by 10 orders to 3.28×10^{-5} S cm^{-1}. However, the conductivity of the epoxy composite filled with 0.5 wt% untreated graphene (about 0.241 vol% of the composite) was only 1.93×10^{-10} S cm^{-1}, which was much lower than that of the composites loaded with 0.5 wt% GA-II/graphene. These results indicated the advantage of the GA/graphene.

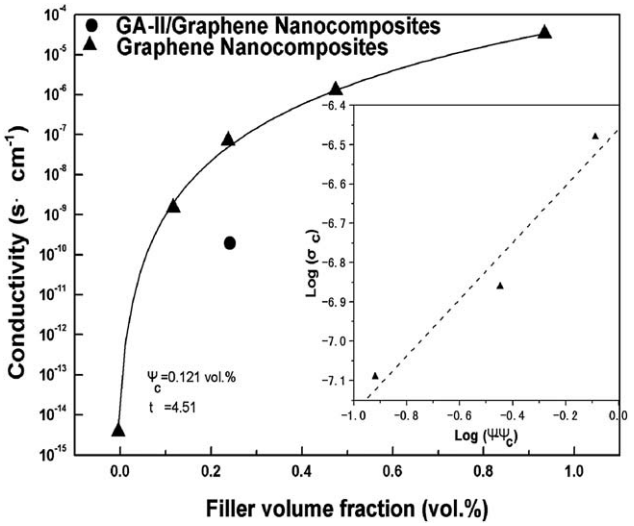

Fig. 7 Electrical conductivity plot for the epoxy/graphene composites.

As we know, a sharp increase in the electrical conductivity of composites takes place only when the continuous conductive network is formed by the addition of conductive fillers. The percolation threshold is the filler content above which a rapid increase of electrical conductivity could be obtained. Based on Fig. 7, the percolation threshold for our system occurred when the filler content reached near 0.121 vol%. To the best of our knowledge, this percolation threshold was lower than the reported values for graphene/epoxy composites.[45] The conductivities of different systems in this study were treated with the following equation:

$$\sigma_e = \sigma_f(\Psi - \Psi_c)^t$$

where σ_e is the conductivity of the nanocomposites, σ_f is the conductivity of the filler, Ψ is the filler volume fraction, Ψ_c is the percolation volume fraction and t is the universal critical exponent. As shown in the inset of Fig. 7 (log–log plot of σ_e *versus* $[\Psi - \Psi_c]$), when $\Psi_c = 0.12\%$ and $t = 4.51$, the experimental results fitted well with the above equation.

4 Conclusions

A bio-based epoxy monomer GA-II was synthesized from renewable gallic acid. Considering its unique chemical structure, it was employed to functionalize graphene *via* π–π interactions so as to inhibit their aggregation and facilitate homogeneous dispersion within an epoxy matrix. Investigation on the thermal conductivity, electrical conductivity as well as the mechanical properties of the composites demonstrated that the bio-based GA-II was a highly efficient dispersing agent for graphene *via* π–π interactions. The graphene composites with superior properties could be fabricated through a more environmentally friendly method, avoiding the chemical modification of graphene or using a bio-based dispersant. The bio-based agent for graphene dispersion was reported for the first time in this work.

Acknowledgements

The authors would like to acknowledge the financial support from Project 51203176 supported by NSFC, Project 51003116 supported by NSFC, the National Basic Research Program of China (973 Program, Grant no. 2010CB631100) and Ningbo Natural Science Foundation (Grant no. 2010A610192, 2011A610127) as well as the Director's Science Foundation of NIMTE.

Notes and references

1 S. Stankovich, D. A. Dikin, G. H. Dommett, K. M. Kohlhaas, E. J. Zimney, E. A. Stach, R. D. Piner, S. T. Nguyen and R. S. Ruoff, *Nature*, 2006, **442**, 282.

2 Y. Zhu, S. Murali, W. Cai, X. Li, J. W. Suk, J. R. Potts and R. S. Ruoff, *Adv. Mater.*, 2010, **22**, 3906.
3 V. Singh, D. Joung, L. Zhai, S. Das, S. I. Khondaker and S. Seal, *Prog. Mater. Sci.*, 2011, **56**, 1178.
4 X. Huang, X. Qi, F. Boey and H. Zhang, *Chem. Soc. Rev.*, 2012, **41**, 666.
5 K. M. F. Shahil and A. A. Balandin, *Nano Lett.*, 2012, **12**, 861.
6 R. Lu, D. Rao, Z. Lu, J. Qian, F. Li, H. Wu, Y. Wang, C. Xiao, K. Deng, E. Kan and W. Deng, *J. Phys. Chem. C*, 2012, **116**, 21291.
7 W. Regan, S. Byrnes, W. Gannett, O. Ergen, O. Vazquez-Mena, F. Wang and A. Zettl, *Nano Lett.*, 2012, **12**, 4300.
8 C. C. Teng, C. C. M. Ma, C. H. Lu, S. Y. Yang, S. H. Lee, M. C. Hsiao, M. Y. Yen, K. C. Chiou and T. M. Lee, *Carbon*, 2011, **49**, 5107.
9 S. Stankovich, D. A. Dikin, R. D. Piner, K. A. Kohlhaas, A. Kleinhammes, Y. Jia, Y. Wu, S. T. Nguyen and R. S. Ruoff, *Carbon*, 2007, **45**, 1558.
10 S. Ansari and E. P. Giannelis, *J. Polym. Sci., Part B: Polym. Phys.*, 2009, **47**, 888.
11 H. Im and J. Kim, *Carbon*, 2012, **50**, 5429.
12 H.-B. Zhang, W.-G. Zheng, Q. Yan, Y. Yang, J.-W. Wang, Z.-H. Lu, G.-Y. Ji and Z.-Z. Yu, *Polymer*, 2010, **51**, 1191.
13 H. Chen, M. B. Müller, K. J. Gilmore, G. G. Wallace and D. Li, *Adv. Mater.*, 2008, **20**, 3557.
14 J. Mohammad, A. Rafiee, Z. Wang, H. Song, Z.-Z. Yu and N. Koratkar, *ACS Nano*, 2009, **3**, 3884.
15 F. Li, Y. Bao, J. Chai, Q. Zhang, D. Han and L. Niu, *Langmuir*, 2010, **26**, 12314.
16 J. M. Englert, J. Röhrl, C. D. Schmidt, R. Graupner, M. Hundhausen, F. Hauke and A. Hirsch, *Adv. Mater.*, 2009, **21**, 4265.
17 K. S. Subrahmanyam, A. Ghosh, A. Gomathi, A. Govindaraj and C. N. R. Rao, *Nanosci. Nanotechnol. Lett.*, 2009, **1**, 28.
18 S. H. Lee, D. R. Dreyer, J. An, A. Velamakanni, R. D. Piner, S. Park, Y. Zhu, S. O. Kim, C. W. Bielawski and R. S. Ruoff, *Macromol. Rapid Commun.*, 2010, **31**, 281.
19 P. Akcora, S. K. Kumar, J. Moll, S. Lewis, L. S. Schadler, Y. Li, B. C. Benicewicz, A. Sandy, S. Narayanan, J. Ilavsky, P. Thiyagarajan, R. H. Colby and J. F. Douglas, *Macromolecules*, 2009, **43**, 1003.
20 S. Park, D. A. Dikin, S. T. Nguyen and R. S. Ruoff, *J. Phys. Chem. C*, 2009, **113**, 15801.
21 M. Fang, K. Wang, H. Lu, Y. Yang and S. Nutt, *J. Mater. Chem.*, 2009, **19**, 7098.
22 S. Ganguli, A. K. Roy and D. P. Anderson, *Carbon*, 2008, **46**, 806.
23 B. Das, K. E. Prasad, U. Ramamurty and C. N. R. Rao, *Nanotechnology*, 2009, 20.
24 A. S. Wajid, H. S. T. Ahmed, S. F. Irin, A. F. Jankowski and M. J. Green, *Macromol. Mater. Eng.*, 2012, 1.
25 T. E. Graedel and J. A. Howard-Grenville, *Greening the Industrial Facility, Perspectives, Approaches and Tools Springer*, 2005, p. 13.
26 Y. Lei, Z. Tang, R. Liao and B. Guo, *Green Chem.*, 2011, **13**, 1655.
27 D. Lin, N. Liu, K. Yang, L. Zhu, Y. Xu and B. Xing, *Carbon*, 2009, **47**, 2875.
28 B. Shen, W. Zhai, C. Chen, D. Lu, J. Wang and W. Zheng, *ACS Appl. Mater. Interfaces*, 2011, **3**, 3103.
29 A. Peigney, C. Laurent, E. Flahaut, R. R. Bacsa and A. Rousset, *Carbon*, 2001, **39**, 507.
30 P. S. Sane, D. V. Palaskar and P. P. Wadgaonkar, *Eur. Polym. J.*, 2011, **47**, 1621.
31 Y. Kishi, S. Sugiura, H. Tanino, T. Goto, M. Aratani, H. Kakoi, S. Inoue and T. Fukuyama, *J. Chem. Soc., Dalton Trans.*, 1972, 64.
32 M. Degirmenci, A. Acikses and N. Genli, *J. Appl. Polym. Sci.*, 2012, **123**, 2567.
33 C. Aouf, H. Nouailhas, M. Fache, S. Caillol, B. Boutevin and H. Fulcrand, *Eur. Polym. J.*, DOI: 10.1016/j.eurpolymj.2012.11.025.
34 C. Aouf, J. Lecomte, P. Villeneuve, E. Dubreucq and H. Fulcrand, *Green Chem.*, 2012, **14**, 2328.
35 A. C. Ferrari, J. C. Meyer, V. Scardaci, C. Casiraghi, M. Lazzeri, F. Mauri, S. Piscanec, D. Jiang, K. S. Novoselov, S. Roth and A. K. Geim, *Phys. Rev. Lett.*, 2006, **97**, 187401.
36 Q. Su, S. Pang, V. Alijani, C. Li, X. Feng and K. Müllen, *Adv. Mater.*, 2009, **21**, 3191.
37 V. Z. Poenitzsch, D. C. Winters, H. Xie, G. R. Dieckmann, A. B. Dalton and I. H. Musselman, *J. Am. Chem. Soc.*, 2007, **129**, 14724.
38 J. Zhu, B. S. Shim, M. Di Prima and N. A. Kotov, *J. Am. Chem. Soc.*, 2011, **133**, 7450.
39 G. A. Rance, D. H. Marsh, R. J. Nicholas and A. N. Khlobystov, *Chem. Phys. Lett.*, 2010, **493**, 19.
40 S. Kamada, H. Nomoto, K. Fukuda, T. Fukawa, H. Shirai and M. Kimura, *Colloid Polym. Sci.*, 2011, **289**, 925.
41 Y. Liang, D. Wu, X. Feng and K. Müllen, *Adv. Mater.*, 2009, **21**, 1679.
42 H. D. Pham, V. H. Pham, T. V. Cuong, T. D. Nguyen-Phan, J. S. Chung, E. W. Shin and S. Kim, *Chem. Commun.*, 2011, **47**, 9672.
43 H. Bai, Y. Xu, L. Zhao, C. Li and G. Shi, *Chem. Commun.*, 2009, 1667.
44 A. J. Patil, J. L. Vickery, T. B. Scott and S. Mann, *Adv. Mater.*, 2009, **21**, 3159.
45 I. Zaman, H.-C. Kuan, Q. Meng, A. Michelmore, N. Kawashima, T. Pitt, L. Zhang, S. Gouda, L. Luong and J. Ma, *Adv. Funct. Mater.*, 2012, **22**, 2735.

